Teichmüller Shape Space Theory and its Application to Brain Morphometry

Yalin Wang[1,2], Wei Dai[3], Xianfeng Gu[4], Tony F. Chan[2], Shing-Tung Yau[5], Arthur W. Toga[1], and Paul M. Thompson[1]

[1] Lab. of Neuro Imaging, UCLA School of Medicine, Los Angeles, CA 90095, USA,
[2] Mathematics Department, UCLA, Los Angeles, CA 90095, USA,
[3] Mathematics Department, Zhejiang Univ. Hangzhou, China,
[4] Comp. Sci. Department, SUNY at Stony Brook, Stony Brook, NY 11794, USA,
[5] Department of Mathematics, Harvard University, Cambridge, MA 02138, USA,
{ylwang}@loni.ucla.edu

Abstract. Here we propose a novel method to compute Teichmüller shape space based shape index to study brain morphometry. Such a shape index is intrinsic, and invariant under conformal transformations, rigid motions and scaling. We conformally map a genus-zero open boundary surface to the Poincaré disk with the Yamabe flow method. The shape indices that we compute are the lengths of a special set of geodesics under hyperbolic metric. Tests on longitudinal brain imaging data were used to demonstrate the stability of the derived feature vectors. In leave-one-out validation tests, we achieved 100% accurate classification (versus only 68% accuracy for volume measures) in distinguishing 11 HIV/AIDS individuals from 8 healthy control subjects, based on Teichmüller coordinates for lateral ventricular surfaces extracted from their 3D MRI scans.

1 Introduction

In the computational analysis of brain anatomy, volumetric measures of structure identified on 3D MRI have been used to study group differences in brain structure and also to predict diagnosis [1]. Recent work has also used shape-based features [2] to analyze surface changes. In research studies that analyze brain morphometry, many shape analysis methods have been proposed, such as spherical harmonic analysis (SPHARM) [3], medial representations (M-reps) [4], and minimum description length approaches [5], etc.; these methods may be applied to analyze shape changes or abnormalities in subcortical brain structures. Even so, a stable method to compute transformation-invariant shape descriptors would be highly advantageous in this research field. Here we propose a novel and intrinsic method to compute surface Teichmüller space coordinates (shape indices) and we apply it to study brain morphometry in Alzheimers disease (AD) and HIV/AIDS. The computed Teichmüller space coordinates are based on the surface conformal structure and can be accurately computed using the Yamabe flow method.

There are extensive research on brain surface conformal parameterization [6–11]. All surfaces may be classified by the conformal equivalence relation. If there

exists a conformal map between two surfaces, then they are conformally equivalent. Any two conformally equivalent surfaces have the same conformal invariants and the same Teichmüller space coordinates. By computing and studying Teichmüller space coordinates and their statistical behavior, we can provide a promising approach to describe local changes or abnormalities in anatomical morphometry due to disease or development.

In this work, only genus-zero surfaces with three boundaries are considered. With the discrete surface Ricci flow method [10] (also called the discrete Yamabe flow), we conformally projected the surfaces to the hyperbolic plane and isometrically embedded them in the Poincaré disk. The proposed Teichmüller space coordinates are the lengths of a special set of geodesics under this special hyperbolic metric and can index and compare general surfaces. To the best of our knowledge, it is the first work to apply the Teichmüller space theory to brain morphometry research. For the cerebral cortex surface, first, we converted a closed 3D surface model of the cerebral cortex into a multiple-boundary surface by cutting it along selected anatomical landmark curves. Secondly, we conformally parameterized each cortical surface using the Yamabe flow method. Next, we computed the Teichmüller space coordinates - the lengths of three boundaries (geodesics) on the hyperbolic space - as a 3×1 feature vector. This measure is invariant in the hyperbolic plane under conformal transformations of the original surface, and is the same for surfaces that differ at most by a rigid motion.

We tested our algorithm on cortical and lateral ventricular surfaces extracted from 3D anatomical brain MRI scans. We tested our algorithms on brain longitudinal data to demonstrate the stability of our proposed Teichmüller space coordinate features. Finally, we used a nearest-neighbor classifier together with our feature vector on the lateral ventricular surface data from a group of 11 HIV/AIDS individuals and a group of 8 matched healthy control subjects. Our classifier achieved a 100% accuracy rate and outperformed a nearest neighbor classifier based on lateral ventricle volumes, which achieved an overall 68.42% accuracy rate on the same dataset.

2   Computational Algorithms

This section briefly introduces the computational algorithms in the current work. The theoretic background and definitions were abbreviated due to the page limit. For details, we refer readers to [12] for algebraic topology and [13] for differential geometry.

In this work, only genus-zero surfaces with three boundaries are considered, which are also called as *topological pants*. Let $(S, \mathbf{g})$ be a pair of topological pants with a Riemannian metric $\mathbf{g}$, with three boundaries $\partial S = \gamma_1 + \gamma_2 + \gamma_3$. Let $\tilde{\mathbf{g}}$ be the uniformization metric of S, such that the Gaussian curvature is equal to -1 at every interior point, and the boundaries are geodesics. If the length of the boundary γ_i is l_i under the uniformization metric, then (l_1, l_2, l_3) are the Teichmüller coordinates of S in the Teichmüller space of all conformal classes of a pair of pants. Namely, if two surface share the same Teichmüller coordinates, they can be conformally mapped to each other.

Figure 1(a) illustrates a pair of pants with the hyperbolic metric and its embedding in Poincaré disk, such that the three boundaries, γ_i, are geodesics. The τ_i are the shortest geodesics connecting γ_j, γ_k, so τ_i is orthogonal to both γ_j and γ_k. The γ_i are divided to two segments with equal lengths by τ_j, τ_k. τ_1, τ_2 and τ_3 split the surface to two identical hyperbolic hexagons, with edge lengths $\frac{\gamma_1}{2}, \tau_3, \frac{\gamma_2}{2}, \tau_1, \frac{\gamma_3}{2}, \tau_2$. Furthermore, all the internal angles are right angles. The lengths of τ_1, τ_2, τ_3 are determined by $\gamma_1, \gamma_2, \gamma_3$. For the mapping in Figure 1(a) to be made, the pair of pants can have any geometry, as long as it has the topology shown. It helps us to study general brain anatomical structures.

In practice, most surfaces are approximated by discrete triangular meshes. Let M be a two-dimensional simplicial complex. We denote the set of vertices, edges and faces by V, E, F respectively. We call the *ith* vertex v_i; edge $[v_i, v_j]$ runs from v_i to v_j; and the face $[v_i, v_j, v_k]$ has its vertices sorted counter-clockwise. Figure 1(b) shows the hyperbolic triangle, and its associated edge lengths l_i, y_i, corner angles θ_i and conformal factors u_i.

A *discrete metric* is a function $l : E \rightarrow \mathbb{R}^+$, such that triangle inequality holds on every face, which represents the edge lengths. In this work, we assume all faces are hyperbolic triangles. The *discrete curvature* $K : V \rightarrow \mathbb{R}$ is defined as the angle deficit, i.e., 2π minus the surrounding corner angles for an interior vertex, and π minus the surrounding corner angles for a boundary vertex.

Discrete conformal deformation. Suppose the mesh is embedded in $\mathbb{R}^3$, so it has the induced Euclidean metric. We use l_{ij}^0 to denote the initial induced Euclidean metric on edge $[v_i, v_j]$.

Let $u : V \rightarrow \mathbb{R}$ be the *discrete conformal factor*. The discrete conformal metric deformation, shown in Figure 1(b), is defined as $\sinh(\frac{y_k}{2}) = e^{u_i} \sinh(\frac{l_k}{2}) e^{u_j}$. The *discrete Yamabe flow* is defined as $\frac{du_i}{dt} = -K_i$, where K_i is the curvature at the vertex v_i.

Let $\mathbf{u} = (u_1, u_2, \cdots, u_n)$ be the conformal factor vector, where n is the number of vertices, and $\mathbf{u_0} = (0, 0, \cdots, 0)$. Then the *discrete hyperbolic Yamabe energy* is defined as $E(\mathbf{u}) = \int_{\mathbf{u_0}}^{\mathbf{u}} \sum_{i=1}^n K_i du_i$.

The differential 1-form $\omega = \sum_{i=1}^n K_i du_i$ is closed. We use c_k to denote $\cosh(y_k)$. By direct computation, it can be shown that on each triangle, $\frac{\partial \theta_i}{\partial u_j} = A \frac{c_i + c_j - c_k - 1}{c_k + 1}$, where $A = \frac{1}{\sin(\theta_k) \sinh(y_i) \sinh(y_j)}$, which is symmetric in i, j, so $\frac{\partial \theta_i}{\partial u_j} = \frac{\partial \theta_j}{\partial u_i}$.

It is easy to see that $\frac{\partial K_i}{\partial u_j} = \frac{\partial K_j}{\partial u_i}$, which implies $d\omega = 0$. The discrete hyperbolic Yamabe energy is convex. The unique global minimum corresponds to the hyperbolic metric with zero vertex curvatures. This requires us to compute the Hessian matrix of the energy. The explicit form is given as follows: $\frac{\partial \theta_i}{\partial u_i} = -A \frac{2c_i c_j c_k - c_j^2 - c_k^2 + c_i c_j + c_i c_k - c_j - c_k}{(c_j + 1)(c_k + 1)}$.

The Hessian matrix (h_{ij}) of the hyperbolic Yamabe energy can be computed explicitly. Let $[v_i, v_j]$ be an edge, connecting two faces $[v_i, v_j, v_k]$ and $[v_j, v_i, v_l]$. Then the edge weight is defined as $h_{ij} = \frac{\partial \theta_i^{jk}}{\partial u_j} + \frac{\partial \theta_i^{lj}}{\partial u_j}$; also for $h_{ii} = \sum_{j,k} \frac{\partial \theta_i^{jk}}{\partial u_i}$,

where the summation goes through all faces surrounding v_i, $[v_i, v_j, v_k]$. The discrete hyperbolic energy can be directly optimized using Newton's method. Because the energy is convex, the optimization process is stable.

Given the mesh M, a conformal factor vector $\mathbf{u}$ is *admissible* if the deformed metric satisfies the triangle inequality on each face. The space of all admissible conformal factors is not convex. In practice, the step length in Newton's method needs to be adjusted. Once the triangle inequality no longer holds on a face, then an edge swap needs to be performed.

3   Experimental Results

We applied our shape analysis to various anatomical surfaces extracted from 3D MRI scans of the brain. In this paper, the segmentations are regarded as given, and result from automated and manual segmentations detailed in other prior works, e.g. Thompson et al. [14, 15].

3.1   Feature Stability Study with Longitudinal Brain Imaging Data

To validate the feasibility and efficiency of our proposed shape index, we compute and compare our shape index on a longitudinal brain imaging dataset [14]. The data set consists of a total of 15 pairs of cortex hemisphere surfaces of individuals with Alzheimer's disease (AD). They were scanned at 2 time points about 2 years apart [14]. AD is characterized by gradual tissue loss throughout the brain; the overall hemisphere volume decreases by around 1 percent per year but it is not known how much change there is in the overall cortical surface shape.

We selected a group of 3 landmark curves per hemisphere: the Central Sulcus, Superior Temporal Sulcus, and Primary Intermediate Sulcus. After we cut a cortical surface open along the selected landmark curves, a cortical surface becomes topologically equivalent to an open boundary genus-2 surface,which is topologically equivalent to the topological pant surface (Figure 1(a)). Figure 1 (c)-(e) illustrate a right hemisphere cortical surface and its embedding in the Poincaré disk. The three boundaries are labeled as γ_i and two shortest geodesics that connect boundaries are labeled as τ_i.

We computed the obtained feature vector for two surfaces, for both the left and right sides of the brain, extracted from the same subject scanned at two different times. For each of 15 subjects, we treated left and right hemisphere brain surfaces equivalently at both time-points, computing shape feature vectors $(T1_i, T2_i), i = 1, ..., 30$, where $T1_i$ and $T2_i$ each is a 3×1 vector. We calculated the L^2 norm of the shape difference for a given cortex hemisphere over time, $d_i = \sqrt{\sum_{j=1}^{3}(T1_{i,j} - T2_{i,j})^2}, i = 1, ..., 30$. For comparison, we also computed the L^2 norm of each feature vector, $l_m, m = 1, ..., 60$. The ratio of the median (d_i) and the median of (l_m) was 0.76%. Although this was a relatively small data set, considerable shape differences were found between different cortical hemispheres. The relatively small difference over time demonstrated the relative stability and efficiency of our proposed feature vector for brain morphometry research.

3.2 Studying Lateral Ventricular Surface Morphometry

The lateral ventricles - fluid-filled structures deep in the brain - are often enlarged in disease and can provide sensitive measures of disease progression [15–18]. Ventricular changes reflect atrophy in surrounding structures; however, the concave shape, complex branching topology and narrowness of the inferior and posterior horns have made automatic analysis more difficult. To model the lateral ventricular surface, we introduced three cuts on each ventricle (*topology optimization*), in which several horns are joined together at the ventricular "atrium" or "trigone" . After modeling the topology in this way, a lateral ventricular surface, in each hemisphere, becomes an open boundary surface with 3 boundaries, a topological pant surface (Figure 1(a)).

Figure 1 (f)-(h) illustrates how to compute Teichmüller space coordinates for a lateral ventricle. In Panel (f) and (g), γ_1, γ_2, and γ_3 are labeled boundaries and τ_1 and τ_2 are the shortest geodesics between boundaries. Panel (h) illustrates the surface with the hyperbolic metric that is isometrically flattened onto the Poincaré disk. When we make the topological change, we make sure each new boundary has the same Euclidean length across different surface. As a result, the lengths of each boundary under the Poincaré disk metric are valid metrics for studying lateral ventricular surface morphometry.

In our experiments, we compared ventricular surface models extracted from 3D brain MRI scans of 11 individuals with HIV/AIDS and 8 control subjects. The data was from a prior work [15]. The data collection, MRI image processing and surface construction were done then. We assume the surface data are given in our current work. We automatically perform topology optimization on each ventricular surface and compute their lengths in the Poincaré disk by the Yamabe flow method. For each pair of ventricular surfaces, we obtained a 6×1 vector, $t = (t_1, t_2, ...t_6)$, which consists of 3 boundary lengths for the left ventricular surface and 3 boundary lengths for right ventricular surface. Given this Teichmüller space coordinate based feature vector, we apply a nearest neighbor classifier based on the Mahalanobis distance, $d(t) = \sqrt{(t - \mu_{T_c})^T \Sigma_{T_c}^{-1}(t - \mu_{T_c})} - \sqrt{(t - \mu_{T_a})^T \Sigma_{T_a}^{-1}(t - \mu_{T_a})}$, where μ_{T_c}, μ_{T_a}, Σ_{T_c} and Σ_{T_a} are the feature vector mean and covariance for the two groups, respectively. We classify t based on the sign of the distance of $d(t)$, i.e., the subject that is closer to one group mean is classified into that group. For this data set, we performed a leave-one-out test. Our classifier successfully classified all 19 subjects to the correct group and achieved a 100% accuracy rate.

For comparison, we also tested a nearest neighbor classifier associated with a volume feature vector. For each pair of ventricular surface, we measure their volumes, (v_l, v_r). We also use a nearest neighbor classifier based on the Mahalanobis distance. We classify v based on the sign of the distance, i. e., the subject that is closer to one group mean is classified into that group. In the same data set, we performed a leave-one-out test. The classifier based on the simple volume measurement successfully classified only 13 out of 19 subjects to the correct group and achieved a 68.42% accuracy rate.

The new Teichmüller space shape descriptor requires more validation on other data sets. However, these experimental results suggest that (1) ventricular surface morphometry is altered in HIV/AIDS; (2) volume measures are not sufficient to distinguish HIV patients from controls; and (3) our Teichmüller space feature vector can be used to classify control and patient subjects. Our ongoing work is studying the correlation between the proposed feature vector and clinical measures (e.g., future decline) in an Alzheimer's Disease data set [18].

4   Discussion

An important step in our algorithm is the topology change, i.e. we cut open surfaces along certain curves. It turns a closed surface into a genus-zero open boundary surface that is topologically equivalent to the topological pant surface in Figure 1(a). In our work, they have strong clinical motivations. In modeling the brain's lateral ventricles (which split in a Y-shape), the anatomical motivation is that we introduce cuts at the ends of the anterior, posterior, and inferior horns, which join at the ventricular "atrium" or "trigone" (the center of the Y-shape). The cuts - where the 3 horns join - are automatically located. For the cortical surface, we select landmark curves that consistently appear in all subjects. An automatic algorithm can locate the landmarks as inputs for the cortex work. There are at least two benefits for us to make topology change. First, the cutting boundaries serve as landmark curves for a consistent comparison across surfaces. Secondly, with the introduced artificial cuts, it is possible for us to compute a global conformal parameterization from the entire surface to the hyperbolic space. In the hyperbolic space, we can conveniently compute shape index that continuously depends on the original surface conformal structure. In some sense, it is similar to Fast Fourier Transform (FFT) for signal processing. Our work can discriminate surface structures by computing a valid shape index from the hyperbolic conformal parameterization.

Our algorithm is based on solving elliptic partial differential equations, so the computation is stable. The computation is also insensitive to the surface triangular mesh quality so it is robust to the digitization errors in the 3D surface reconstruction. Overall, it provides an intrinsic and stable way to compute surface conformal structure based shape index for further morphometry study. For a genus zero surface, if we cut along three individual curves on a surface, we achieve a genus-zero surface with three boundaries. The shape index consists of the geodesic lengths ($\gamma_i, i = 1 - 3$) under the hyperbolic metric in the Poincaré disk. The boundaries are clinically motivated and easy to find automatically; the shape feature is purely determined by the major anatomical features, which are easily identified and consistent across surfaces. For both applications, the shape index is determined by the overall shape so it is not very sensitive to changes in a small neighborhood. Any closed anatomical structure surfaces can be modeled in this way and becomes a topologically equivalent to a topological pant surface. Even we only consider the topological pant surface here, our method is general and can handle all arbitrary topology surfaces with negative Euler numbers. In

future, we will explore more general surface applications and compare it with other shape-based surface measures.

References

1. C. M. Botino, C. C. Castro, R. L. Gomes, C. A. Buchpiguel, R. L. Marchetti, and M. R. Neto. Volumetric MRI measurements can differentiate Alzheimer's disease, mild cognitive impairment and nomral aging. *International Psychogeriatrics*, 14:59–72, 2002.
2. S. Li, F. Shi, F. Pu, X. Li, T. Jiang, S. Xie, and Y. Wang. Hippocampal shape analysis of Alzheimer's disease based on machine learning methods. *American J. of Neuroradiology*, 28:1339–45, 2007.
3. M.K. Chung, K.M. Dalton, and R.J. Davidson. Tensor-based cortical surface morphometry via weighted spherical harmonic representation. *IEEE Trans. Med. Imag.*, 27(8):1143–1151, Aug. 2008.
4. S.M. Pizer, D.S. Fritsch, P.A. Yushkevich, V.E. Johnson, and E.L. Chaney. Segmentation, registration, and measurement of shape variation via image object shape. *IEEE Trans. Med. Imag.*, 18(10):851–865, Oct. 1999.
5. R. H. Davies, C. J. Twining, P. D. Allen, T. F. Cootes, and C. J. Taylor. Shape discrimination in the hippocampus using an MDL model. In *Proc. Infor. Proc. Med. Imag. (IPMI)*, 2003.
6. M. K. Hurdal and K. Stephenson. Cortical cartography using the discrete conformal approach of circle packings. *NeuroImage*, 23:S119–S128, 2004.
7. S. Angenent, S. Haker, A. Tannenbaum, and R. Kikinis. Conformal geometry and brain flattening. *Med. Image Comput. Comput.-Assist. Intervention*, pages 271–278, Sep. 1999.
8. X. Gu, Y. Wang, T. F. Chan, P. M. Thompson, and S.-T. Yau. Genus zero surface conformal mapping and its application to brain surface mapping. *IEEE Trans. Med. Imag.*, 23(8):949–958, Aug. 2004.
9. Y. Wang, L. M. Lui, X. Gu, K. M. Hayashi, T. F. Chan, A. W. Toga, P. M. Thompson, and S.-T. Yau. Brain surface conformal parameterization using Riemann surface structure. *IEEE Trans. Med. Imag.*, 26(6):853–865, June 2007.
10. Y. Wang, X. Gu, T. F. Chan, P. M. Thompson, and S.-T. Yau. Brain surface conformal parameterization with algebraic functions. *Med. Image Comp. Comput.-Assist. Intervention, Proceedings, Part II*, pages 946–954, 2006. LNCS 4191.
11. Y. Wang, X. Gu, T. F. Chan, P. M. Thompson, and S.-T. Yau. Conformal slit mapping and its applications to brain surface parameterization. *Med. Image Comp. Comput.-Assist. Intervention, Proceedings, Part I*, pages 585–593, 2008. LNCS 5241.
12. Allen Hatcher. *Algebraic Topology*. Camerbirdge University Press, 2006.
13. Heinrich W. Guggenheimer. *Differential Geometry*. Dover Publications, 1977.
14. P. M. Thompson, K. M. Hayashi, G. De Zubicaray, A. L. Janke, S. E. Rose, J. Semple, D. Herman, M. S. Hong, S. S. Dittmer, D. M. Doddrell, and A. W. Toga. Dynamics of gray matter loss in Alzheimer's disease. *J. Neuroscience*, 23:994–1005, 2003.

15. P. M. Thompson, R. A. Dutton, K. M. Hayashi, A. Lu, S. E. Lee, J. Y. Lee, O. L. Lopez, H. J. Aizenstein, A. W. Toga, and J. T. Becker. 3D mapping of ventricular and corpus callosum abnormalities in HIV/AIDS. *NeuroImage*, 2006. In Press.

16. O.T. Carmichael, P.M. Thompson, R.A. Dutton, A. Lu, S.E. Lee, J.Y. Lee, L.H. Kuller, O.L. Lopez, H.J. Aizenstein, C.C. Meltzer, Yanxi Liu, A.W. Toga, and J.T. Becker. Mapping ventricular changes related to dementia and mild cognitive impairment in a large community-based cohort. *Biomedical Imaging: Nano to Macro, 2006. 3rd IEEE International Symposium on*, pages 315–318, April 2006.

17. Luca Ferrarini, Walter M. Palm, Hans Olofsen, Mark A. van Buchem, Johan H.C. Reiber, and Faiza Admiraal-Behloul. Shape differences of the brain ventricles in Alzheimer's disease. *NeuroImage*, 32(3):1060 – 1069, 2006.

18. Yi-Yu Chou, Natasha Lepor, Ming-Chang Chiang, Christina Avedissian, Marina Barysheva, Katie L. McMahon, Greig I. de Zubicaray, Matthew Meredith, Margaret J. Wright, Arthur W. Toga, and Paul M. Thompson. Mapping genetic influences on ventricular structure in twins. *NeuroImage*, 44(4):1312 – 1323, 2009.
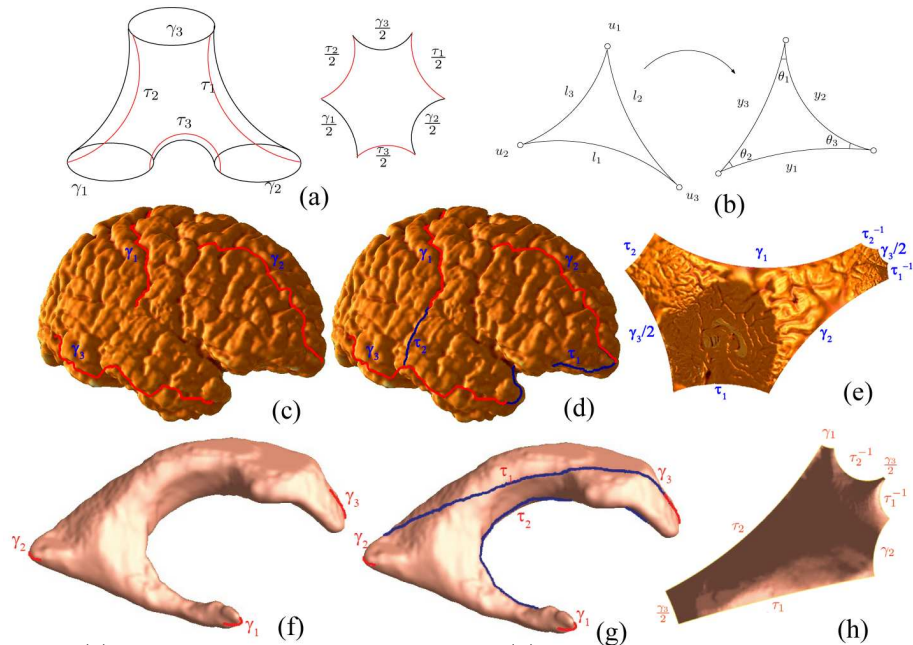
Fig. 1: (a) shows a pair of hyperbolic pants. (b) shows conformal deformation of a hyperbolic triangle. (c)-(e) illustrate how to compute the shape index on a right hemisphere cortical surface with 3 selected landmarks. (f)-(h) illustrate how to compute the shape index on a left ventricular surface. When using it as a feature vector for shape classification, a nearest neighbor classifier achieved a 100% accuracy classification in distinguishing 11 HIV/AIDS individuals from 8 healthy control subjects (versus 68% accuracy for volume measures). The shape index also detected genetic influences more powerfully than volumetric measures in a set of lateral ventricle surfaces from 76 identical twins and 56 same-sex fraternal twins than volume measures.